NASA TECHNICAL MEMORANDUM

NASA TM X-1601

NASA TM X-1601

AERODYNAMIC CHARACTERISTICS OF SEVERAL HYPERSONIC BOOST-GLIDE-TYPE CONFIGURATIONS AT MACH NUMBERS FROM 2.30 TO 4.63

by Ernald B. Graves and Melvin M. Carmel
Langley Research Center
Langley Station, Hampton, Va.

NATIONAL AERONAUTICS AND SPACE ADMINISTRATION • WASHINGTON, D. C. • SEPTEMBER 1968

NASA TM X-1601

AERODYNAMIC CHARACTERISTICS OF SEVERAL HYPERSONIC BOOST-GLIDE-TYPE CONFIGURATIONS AT MACH NUMBERS FROM 2.30 TO 4.63

By Ernald B. Graves and Melvin M. Carmel

Langley Research Center
Langley Station, Hampton, Va.

NATIONAL AERONAUTICS AND SPACE ADMINISTRATION

For sale by the Clearinghouse for Federal Scientific and Technical Information
Springfield, Virginia 22151 – CFSTI price $3.00

AERODYNAMIC CHARACTERISTICS OF SEVERAL HYPERSONIC BOOST-GLIDE-TYPE CONFIGURATIONS AT MACH NUMBERS FROM 2.30 TO 4.63

By Ernald B. Graves and Melvin M. Carmel
Langley Research Center

SUMMARY

An investigation has been conducted at Mach numbers from 2.30 to 4.63 to determine the static aerodynamic characteristics of several configurations designed for flight at hypersonic Mach numbers. Two all-wing and three wing-body configurations were tested through an angle-of-attack range from about -4° to 33° and an angle-of-sideslip range from about -4° to 8° at a Reynolds number of 3×10^6 per foot (9.84×10^6 per meter).

The results of the investigation indicated that the wing-body configurations produced higher values of maximum lift-drag ratio than those produced by the all-wing models. The high wing-body configurations tend to have a self-trimming capability as opposed to that for the low wing-body configurations. Each of the configurations produced a positive dihedral effect that increased with increasing angle of attack and decreased with increasing Mach number. The high wing-body models produced decreasing values of directional stability with increase in angle of attack, whereas the low wing-body models provided increasing values of directional stability with increase in angle of attack.

INTRODUCTION

The National Aeronautics and Space Administration is conducting continuous research, both lifting and nonlifting, on configurations proposed for hypersonic flight. The lifting configuration category includes entry, boost-glide, and hypersonic cruise vehicles. Examples of some of this research may be found in references 1 to 5. Although the mission requirements and design details of these vehicles are different, studies have shown that they are similar to the point that systematic aerodynamic data on any one of these types of vehicles is considered applicable to the design of the other types. In an effort to provide further information in this field of research, tests have been performed on several hypersonic boost-glide type models at Mach numbers from 2.30 to 4.63. These models were selected from a series previously investigated at Mach numbers of 1.41 and 2.01. (See ref. 1.) The models are given the same identification in this paper as they were given in reference 1. Two of the models are all-wing configurations with modified

delta planform; one having a hexagonal cross section, and the other having a diamond cross section. The remaining configurations are wing-body types, including low- and high-wing configurations with a modified delta-wing planform, and a high-wing configuration with an arrow-type planform.

Results presented herein were obtained at angles of attack from about -4° to 33°, at angles of sideslip from about -4° to 8°, and at a Reynolds number of 3×10^6 per foot (9.84×10^6 per meter).

SYMBOLS

The aerodynamic characteristics of the models are referenced to the body system of axes except for the lift and drag components which are referred to the stability system of axes. The coordinate origins are taken at a point 20 inches (0.508 meter) from the model nose along the body axis of symmetry.

The symbols used herein are defined as follows:

b	reference span (see table I)
C_D	drag coefficient, $\frac{\text{Drag}}{qS}$
C_L	lift coefficient, $\frac{\text{Lift}}{qS}$
C_m	pitching-moment coefficient, $\frac{\text{Pitching moment}}{qSx}$
$C_{m,0}$	pitching-moment coefficient at $C_L = 0$
$C_{D,0}$	drag coefficient at zero lift
C_p	pressure coefficient, $\frac{p - p_\infty}{q}$
$C_{L_\alpha} = \frac{\partial C_L}{\partial \alpha}$	about $\alpha = 0^{\circ}$
$C_{m_\alpha} = \frac{\partial C_m}{\partial \alpha}$	about $\alpha = 0^{\circ}$
C_{Y_β}	side-force parameter
C_{n_β}	directional stability parameter
C_{l_β}	effective dihedral parameter

$(L/D)_{max}$ maximum lift-drag ratio

p static pressure in model chamber

p_∞ free-stream static pressure

q free-stream dynamic pressure

M free-stream Mach number

r body radius

S reference area (see table I)

x longitudinal reference length (see table I)

α angle of attack, deg

β angle of sideslip, deg

APPARATUS AND MODELS

Tunnel

Tests were conducted in the high Mach number test section of the Langley Unitary Plan wind tunnel, which is a closed-loop variable-pressure facility. The test section is about 4 feet (1.22 meters) square and about 7 feet (2.13 meters) long. The nozzle leading to the test section is of the asymmetric sliding-block type which permits a continuous variation in Mach number from about 2.3 to 4.7.

Model

Detailed drawings of the test configurations are presented in figure 1. Table I presents a list of the geometric characteristics. Models 4 and 6 are all-wing configurations, whereas the other models are wing-body configurations. Model 4 has an octagonal cross section, and a clipped-delta planform with vertical fins attached. Model 6 has a diamond cross section and a modified delta planform. The forward 20 percent of model 6 has a 5^o deflection up from the model center line. Models 5 and 8 are identical in overall geometry, model 5 being a low delta-wing configuration, and model 8 being a high delta-wing configuration obtained by inverting model 5. Model 7 is a flat-top, high wing-body

configuration with an arrow-type planform, wedge airfoil sections, and negative dihedral near the wing tips. Body coordinates of model 7 are presented in table II.

Tests and Conditions

Tests were conducted at Mach numbers from 2.30 to 4.63 at angles of attack from about -4° to 33°, at angles of sideslip from about -4° to 8°, and at a Reynolds number of 3×10^6 per foot (9.84×10^6 per meter). Forces and moments on the model were measured by means of an internally mounted, six-component electrical strain-gage balance. Pressure in the balance chamber was measured by means of a single static orifice. Transition strips composed of No. 60 sand in 1/16-inch-wide bands were affixed around the nose of each model 1.2 inches from the apex and also 0.4 inch behind the wing leading edge in a streamwise direction. The test-section dewpoint temperature was maintained sufficiently low to avoid any significant condensation effects.

Angles of attack and sideslip were corrected for sting-balance deflections due to aerodynamic loads. Angles of attack were also corrected for tunnel flow angularity.

Drag coefficient data presented in this paper are gross values for each model; that is, no corrections have been made for model chamber pressure. Figure 2, however, shows the magnitude of the chamber pressure coefficients for each model at each test Mach number.

RESULTS AND DISCUSSION

Longitudinal Characteristics

The longitudinal aerodynamic characteristics of the five configurations are presented in figure 3 and summarized in figure 4. The lift and pitching-moment data are reasonably linear with angle of attack for all the models. The models exhibit the expected decrease in lift-curve slope and minimum drag coefficient with increase in Mach number. In addition, all the models show an increase in $(L/D)_{max}$ with increase in Mach number. It should be noted, however, that all the models have substantial base areas for which no adjustments to drag coefficient were made in the data, and at the two higher test Mach numbers significant areas of laminar boundary layer are probably present because of the small-sized grit in the transition strips. Test results indicate that the wing-body configurations (models 5, 7, and 8) produce the higher values of $(L/D)_{max}$ as opposed to the all-wing configurations; however, volumetric differences between the models have not been considered. Model 7, the swept-wing model, has slightly higher $(L/D)_{max}$ values than the other two wing-body models, and, in addition, has the most aft aerodynamic-center location of all the models of the investigation. There are only small effects of Mach number on aerodynamic-center location for all the configurations. The high-wing

configurations, models 7 and 8, produce positive values of $C_{m,0}$, whereas model 5, a low-wing model, produces a negative $C_{m,0}$. The positive $C_{m,0}$ would tend to have a more favorable effect on the trimmed lift-drag ratio than would the negative $C_{m,0}$ by providing a self-trimming capability. (As shown in ref. 1, there is a decrease in $C_{m,0}$ for model 7 with an increase in Mach number.)

Lateral Characteristics

The lateral parameters for the test models are shown in figure 5 as a function of angle of attack. For all the configurations, there is generally a noticeable increase in positive effective dihedral $\left(-C_{l_\beta}\right)$ with increase in angle of attack, whereas an increase in Mach number leads to a decrease in positive effective dihedral. Only model 4, which had a substantial amount of vertical fin area, displayed positive directional stability throughout the angle-of-attack and Mach number ranges. (See fig. 5(a).) However, each of the configurations could probably be made directionally satisfactory through the proper location of vertical surfaces. It may also be noted that the high wing-body configuration (model 8, fig. 5(e)) produces a decrease in C_{n_β} with an increase in α, whereas the low wing-body configuration (model 5, fig. 1(b)) produces an increase in C_{n_β} with an increase in α. It appears that these effects result from side-force changes acting on the forebody since the high-wing model indicates an increase in $-C_{Y_\beta}$ with increase in α, and the low-wing model indicates a decrease in $-C_{Y_\beta}$ with increase in α. These changes in side force are related to the changes in local dynamic pressure in the flow field of the wing which, with increasing angle of attack, would result in an increase in dynamic pressure below the wing and a decrease in dynamic pressure above the wing.

CONCLUSIONS

Tests of two all-wing and three wing-body hypersonic configurations at Mach numbers from 2.30 to 4.63 lead to the following conclusions:

1. The wing-body configurations produced higher values of maximum lift-drag ratio than those produced by the all-wing models.

2. The high wing-body configurations tend to have a self-trimming capability as opposed to that for the low wing-body configurations.

3. Each of the configurations produced a positive dihedral effect that increased with increasing angle of attack and decreased with increasing Mach number.

4. The high wing-body models produced decreasing values of directional stability with increase in angle of attack, whereas the low wing-body models provided increasing values of directional stability with increase in angle of attack.

Langley Research Center,
National Aeronautics and Space Administration,
Langley Station, Hampton, Va., May 20, 1968,
722-01-00-02-23.

REFERENCES

1. Foster, Gerald V.: Static Stability Characteristics of a Series of Hypersonic Boost-Glide Configurations at Mach Numbers of 1.41 and 2.01. NASA TM X-167, 1959.
2. Rainey, Robert W.: Static Stability and Control of Hypersonic Gliders. NACA RM L58E12a, 1958.
3. Anon.: Conference on Hypersonic Aircraft Technology. NASA SP-148, 1967.
4. Rainey, Robert W.; Fetterman, David E., Jr.; and Smith, Robert: Summary of the Static Stability and Control Results of a Hypersonic Glider Investigation. NASA TM X-277, 1960.
5. Fetterman, David E.; McLellan, Charles H.; Jackson, L. Robert; Henry, Beverly Z., Jr.; and Henry, John R.: A Review of Hypersonic Cruise Vehicles. NASA TM X-1276, 1966.

TABLE I.- MODEL GEOMETRIC CHARACTERISTICS

Model 4:		
Length, ft (m)	2.50	(0.762)
Base area, sq ft (m^2)	0.14	(0.013)
Reference dimensions –		
b (span), ft (m)	0.79	(0.24)
x, ft (m)	1.67	(0.51)
S, sq ft (m^2)	1.19	(0.11)
Model 5:		
Length, ft (m)	2.50	(0.762)
Base area, sq ft (m^2)	0.06	(0.006)
Reference dimensions –		
b (span), ft (m)	0.98	(0.30)
x, ft (m)	1.67	(0.51)
S, sq ft (m^2)	1.33	(0.12)
Model 6:		
Length, ft (m)	2.50	(0.762)
Base area, sq ft (m^2)	0.13	(0.012)
Reference dimensions –		
b (span), ft (m)	0.83	(0.25)
x, ft (m)	1.67	(0.51)
S, sq ft (m^2)	1.34	(0.12)
Model 7:		
Length, ft (m)	2.50	(0.762)
Base area, sq ft (m^2)	0.08	(0.007)
Reference dimensions –		
b (span undeflected), ft (m)	1.37	(0.42)
x (mean geometric chord), ft (m)	1.17	(0.36)
S, sq ft (m^2)	1.49	(0.138)
Model 8:		
Length, ft (m)	2.50	(0.762)
Base area, sq ft (m^2)	0.06	(0.005)
Reference dimensions –		
b (span), ft (m)	0.98	(0.30)
x, ft (m)	1.67	(0.51)
S, sq ft (m^2)	1.33	(0.12)

TABLE II.- BODY COORDINATES OF MODEL 7

Distance from nose		Radius, r	
in.	cm	in.	cm
0.000	0.00	0.000	0.00
.529	1.34	.000	.00
.769	1.95	.068	.17
1.029	2.61	.118	.30
1.529	3.88	.198	.50
2.529	6.42	.337	.86
3.529	8.96	.452	1.15
4.529	11.50	.561	1.42
8.529	21.66	.943	2.40
12.529	31.82	1.278	3.25
16.529	41.98	1.586	4.03
20.529	52.14	1.874	4.76
22.529	57.22	2.013	5.11
24.529	62.30	2.156	5.48
25.529	64.84	2.216	5.63
26.772	68.00	2.298	5.84
30.000	76.20	2.298	5.84

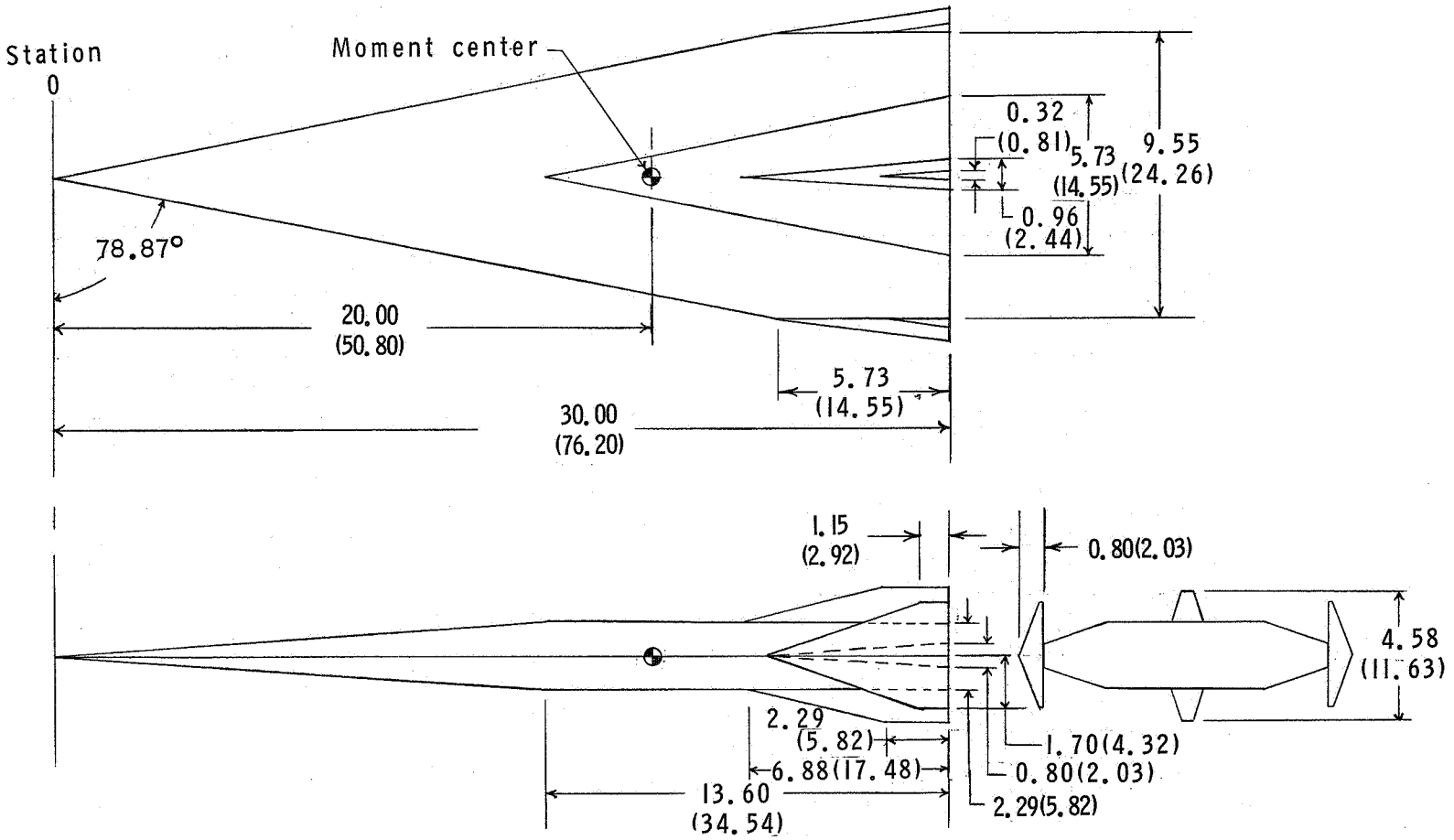

(a) Model 4.

Figure 1.- Details of models. All dimensions are in inches (centimeters) unless otherwise noted.

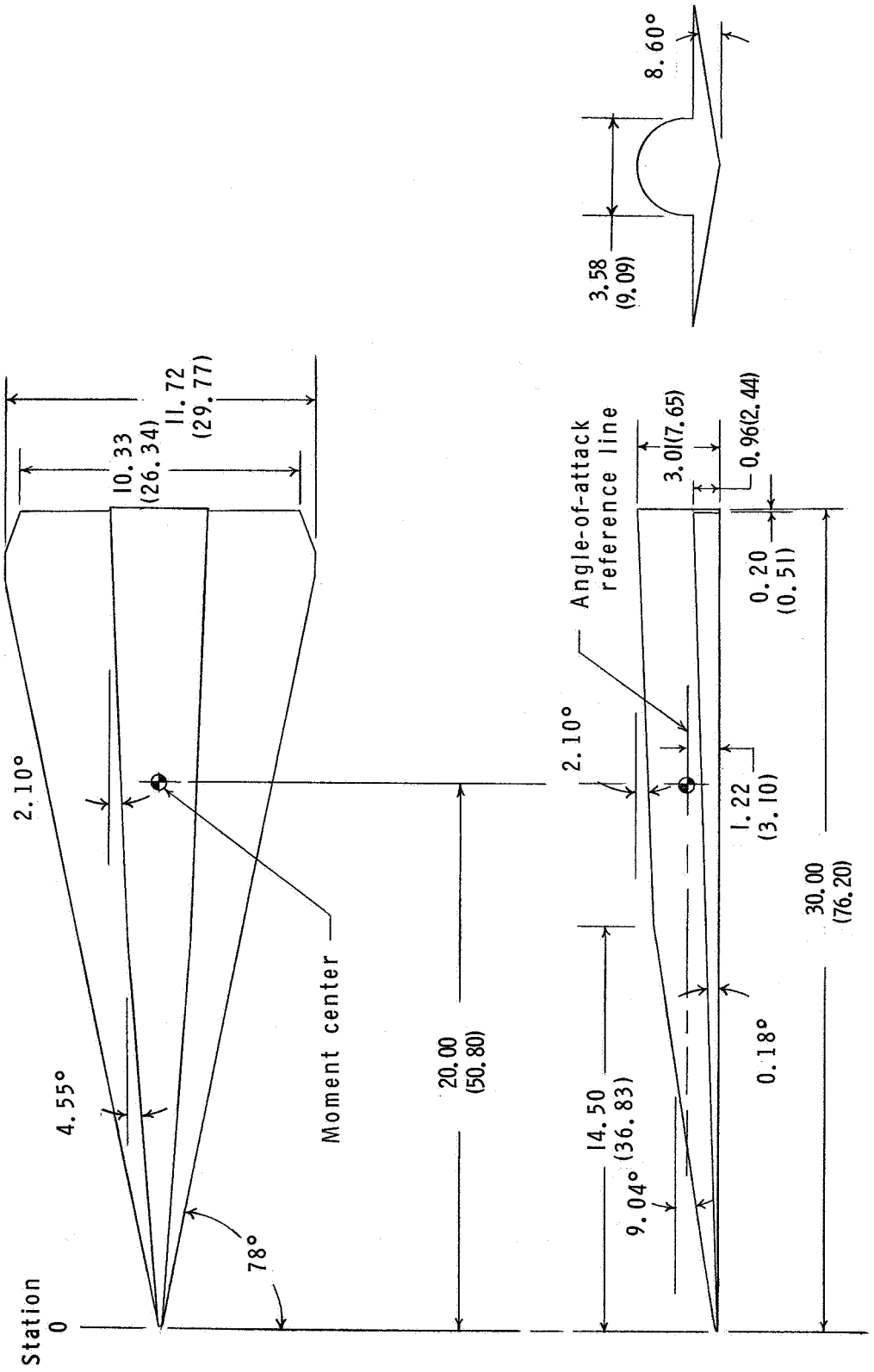

(b) Model 5.

Figure 1.- Continued.

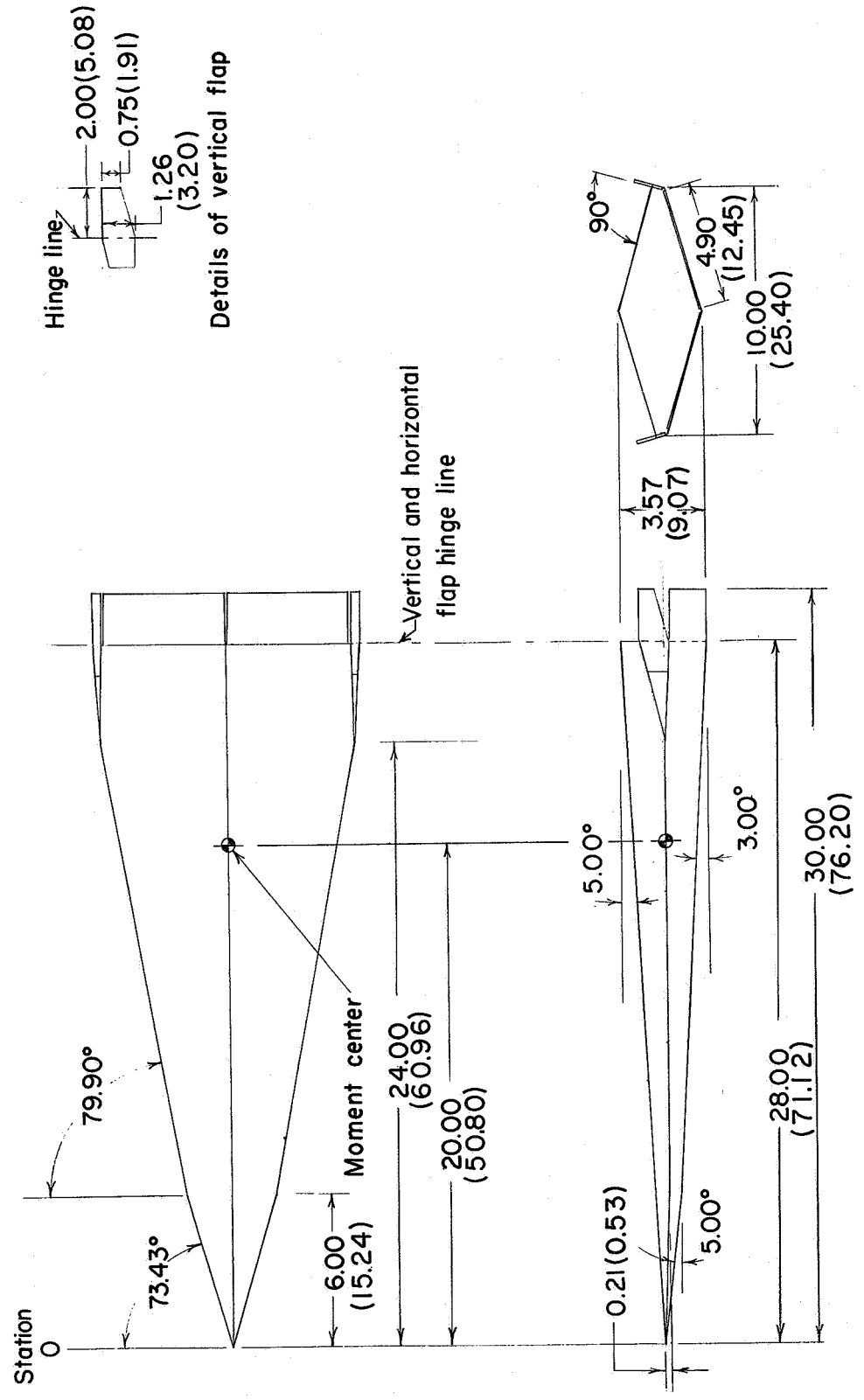

(c) Model 6.

Figure 1.- Continued.

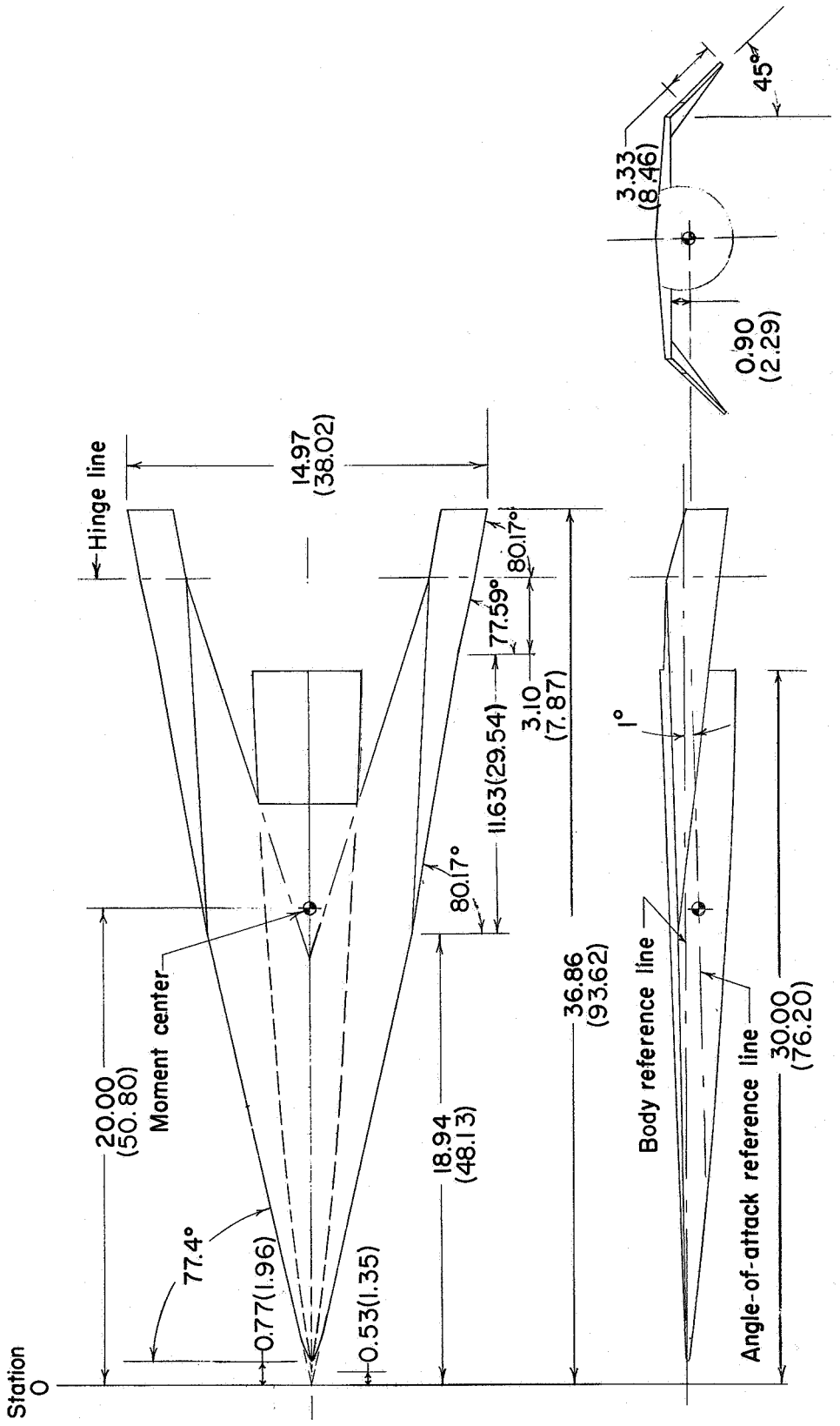

(d) Model 7.

Figure 1.- Continued.

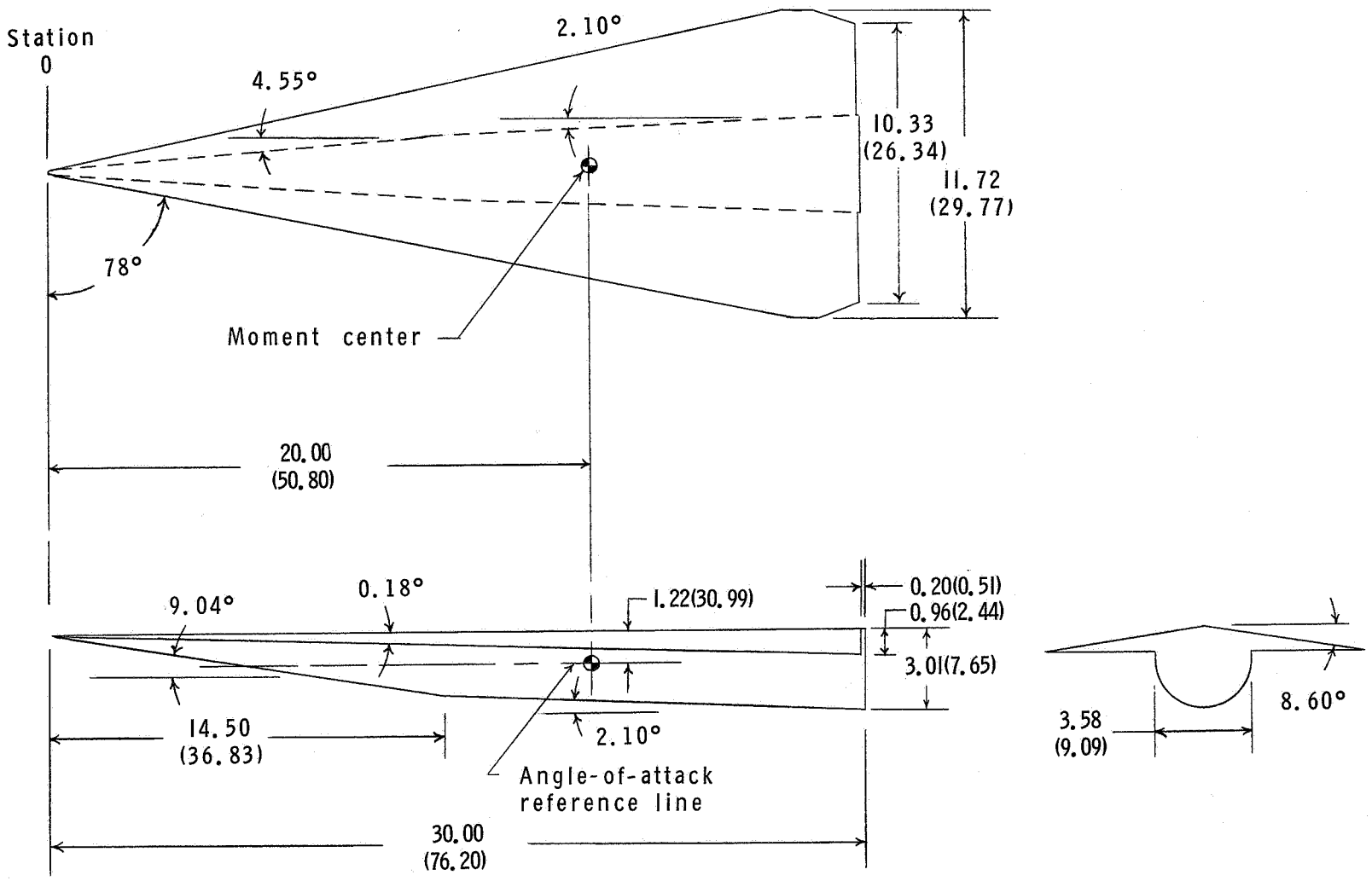

(e) Model 8.

Figure 1.- Concluded.

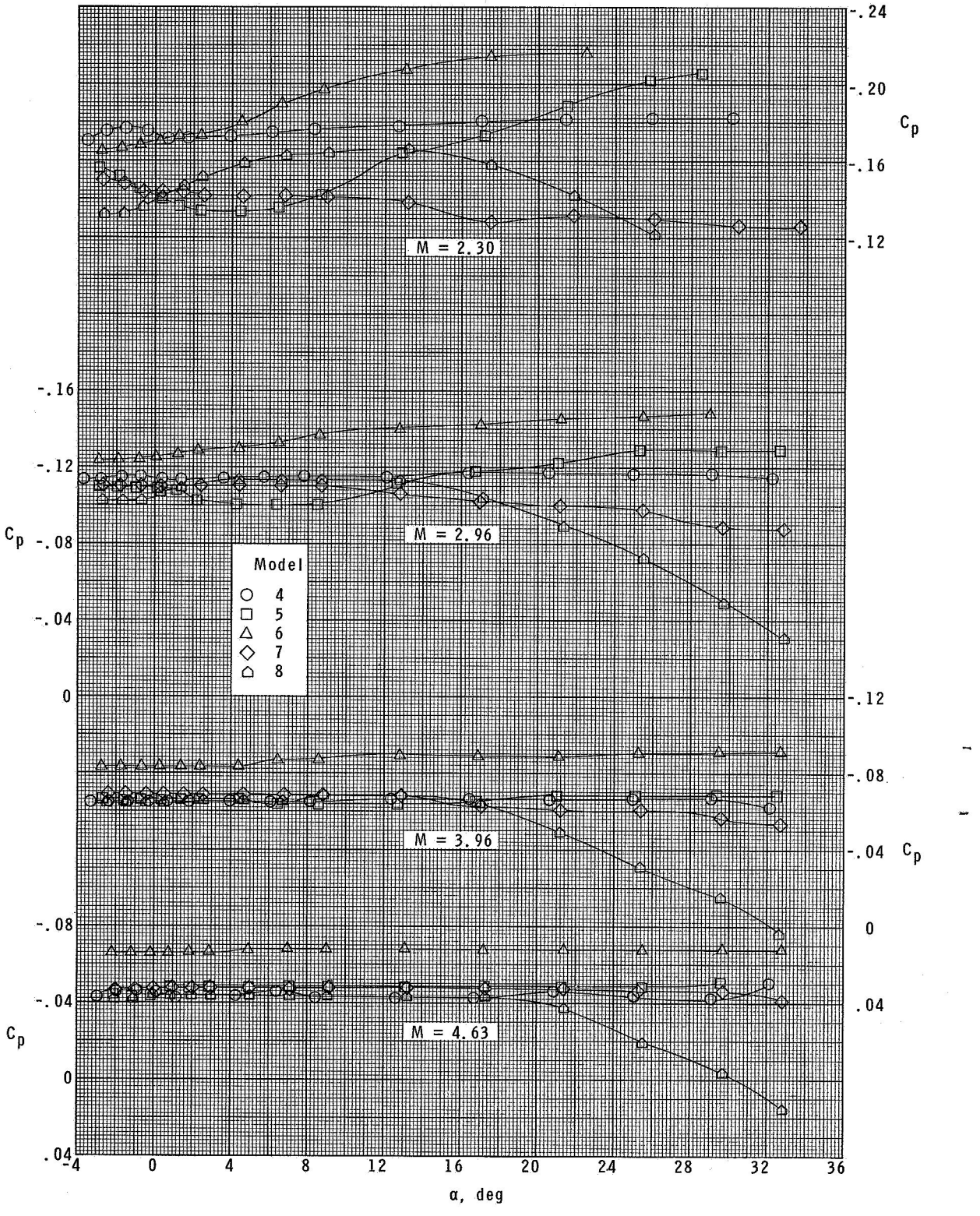

Figure 2.- Variation of chamber pressure coefficient with angle of attack.

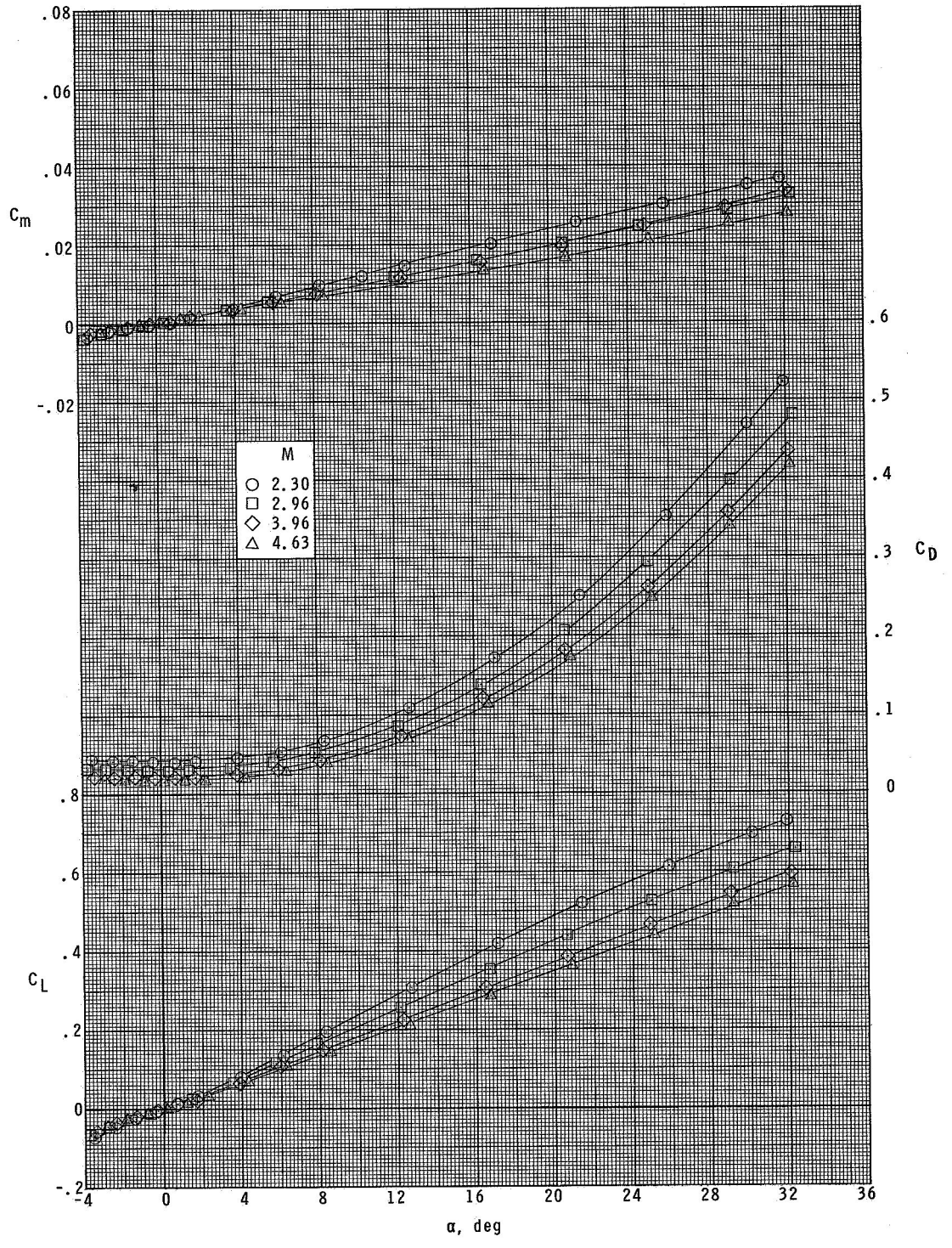

(a) Model 4.

Figure 3.- Variation of aerodynamic characteristics with angle of attack.

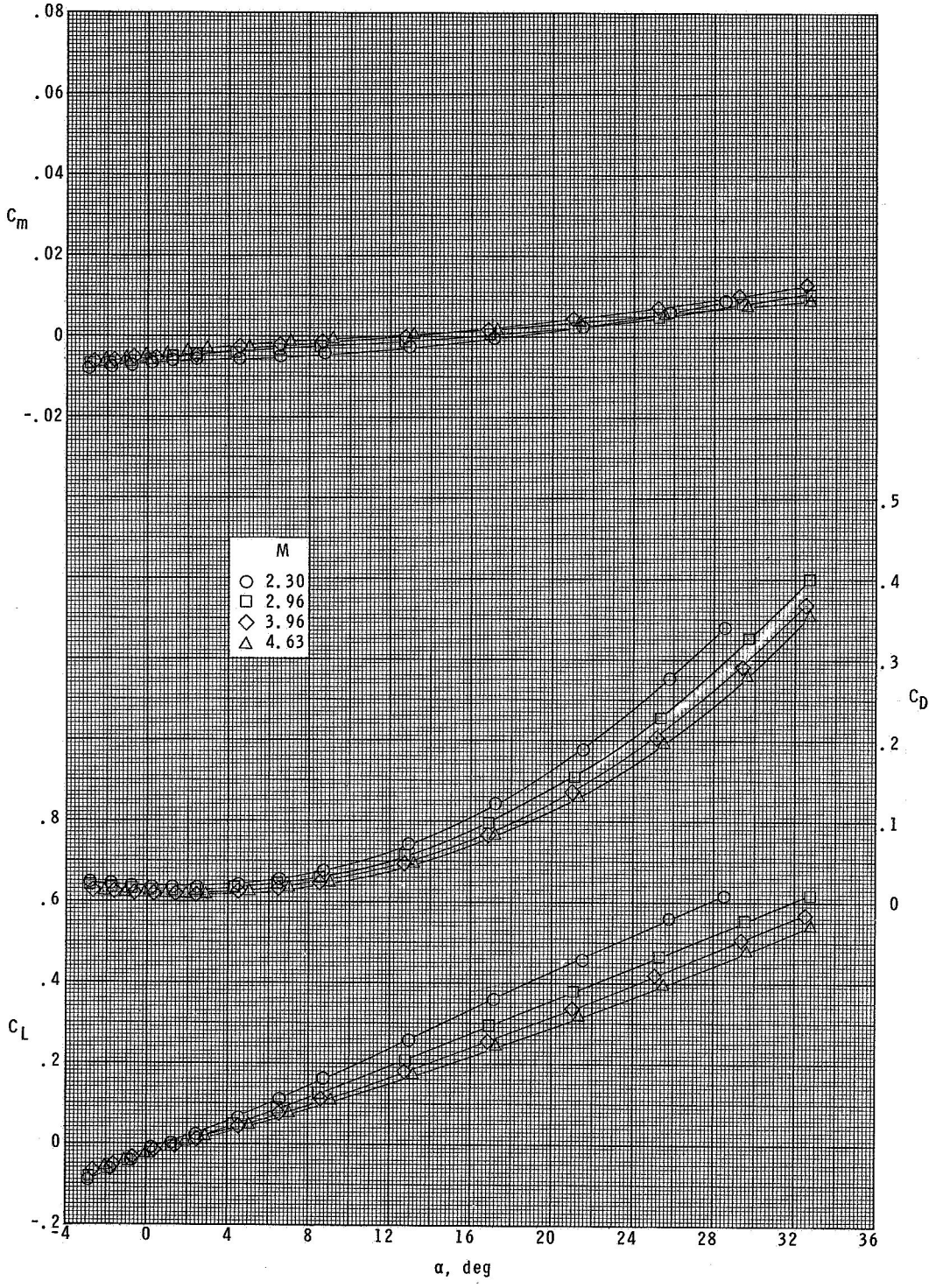

(b) Model 5.

Figure 3.- Continued.

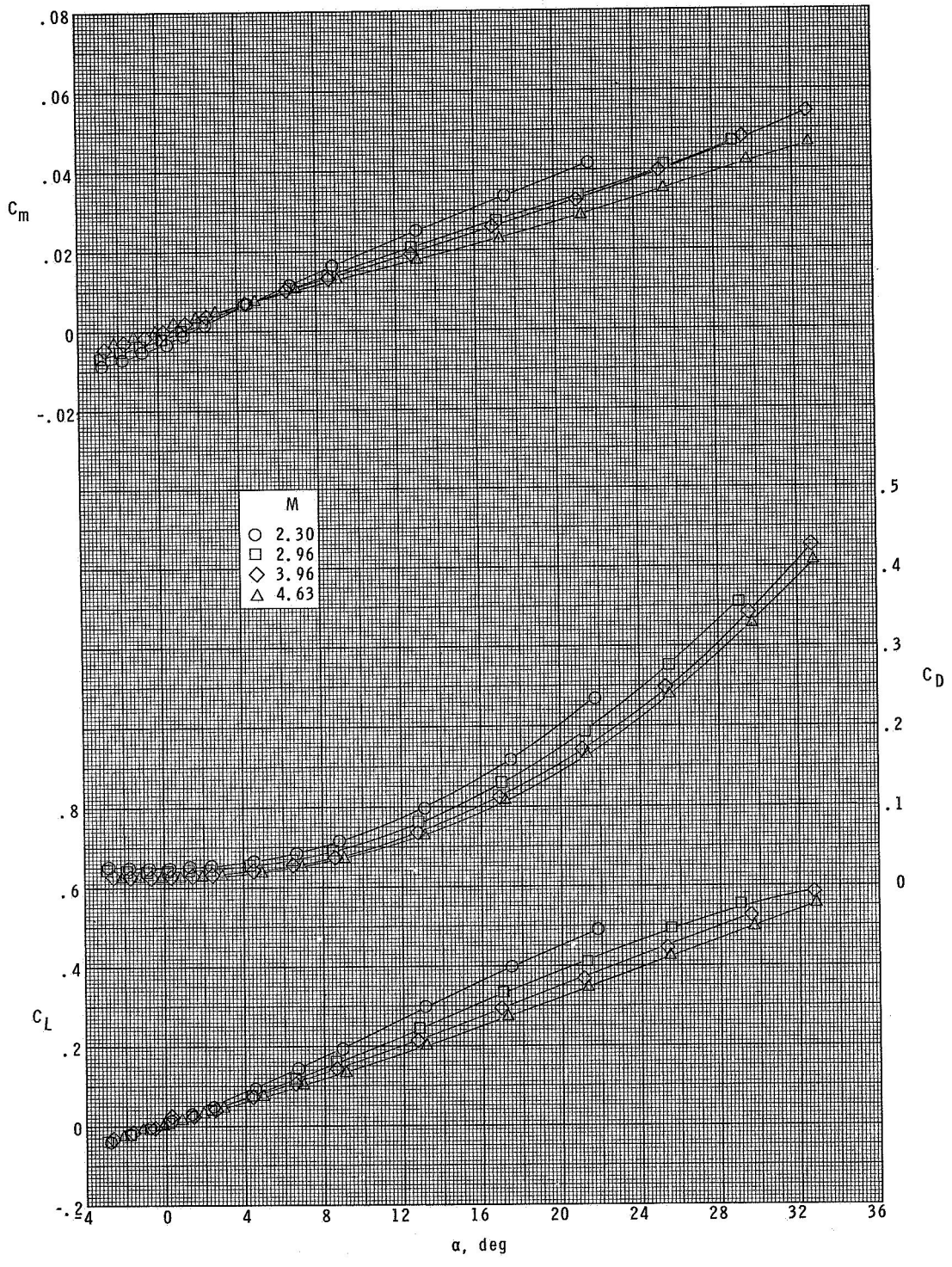

(c) Model 6.

Figure 3.- Continued.

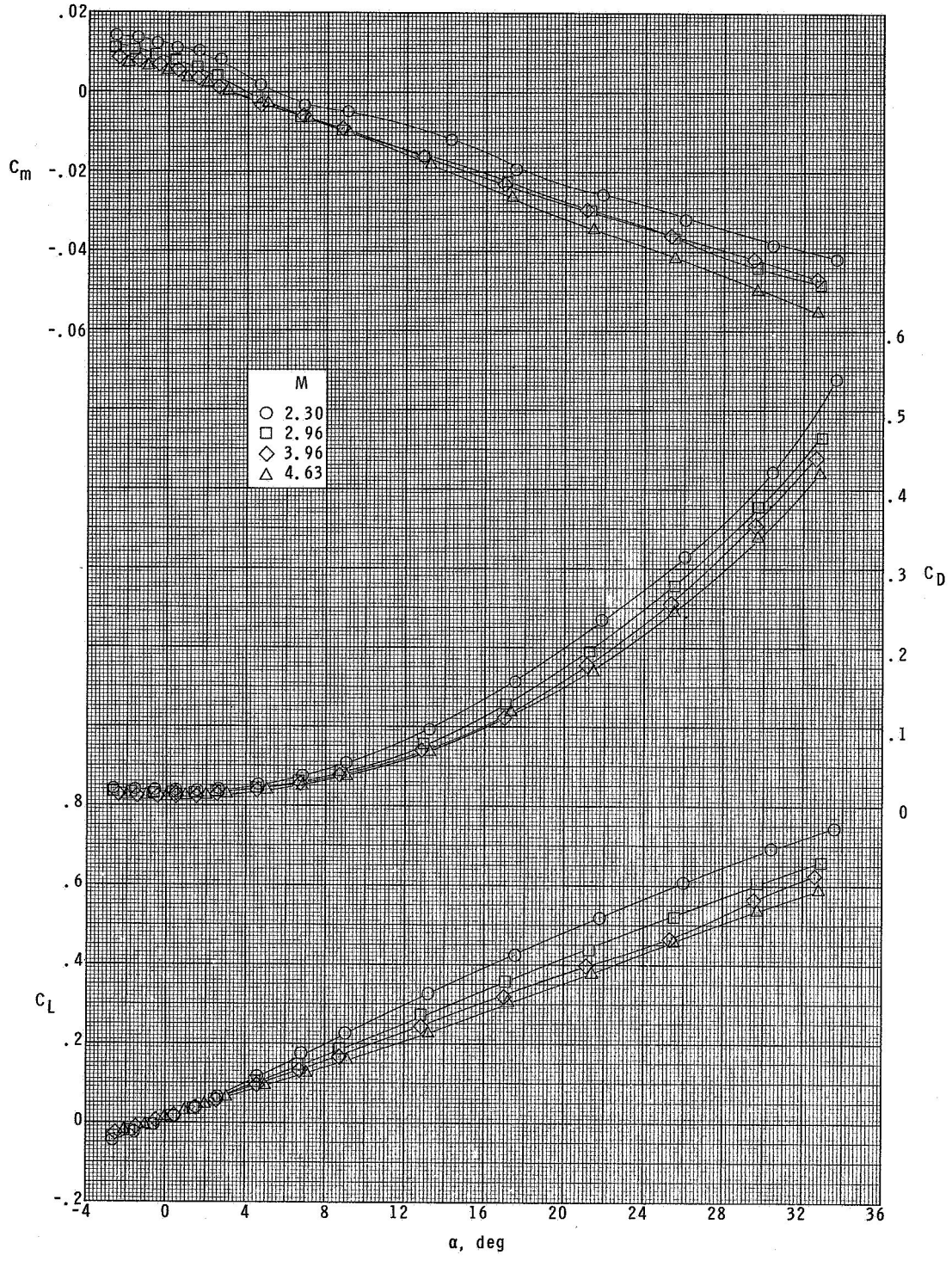

(d) Model 7.

Figure 3.- Continued.

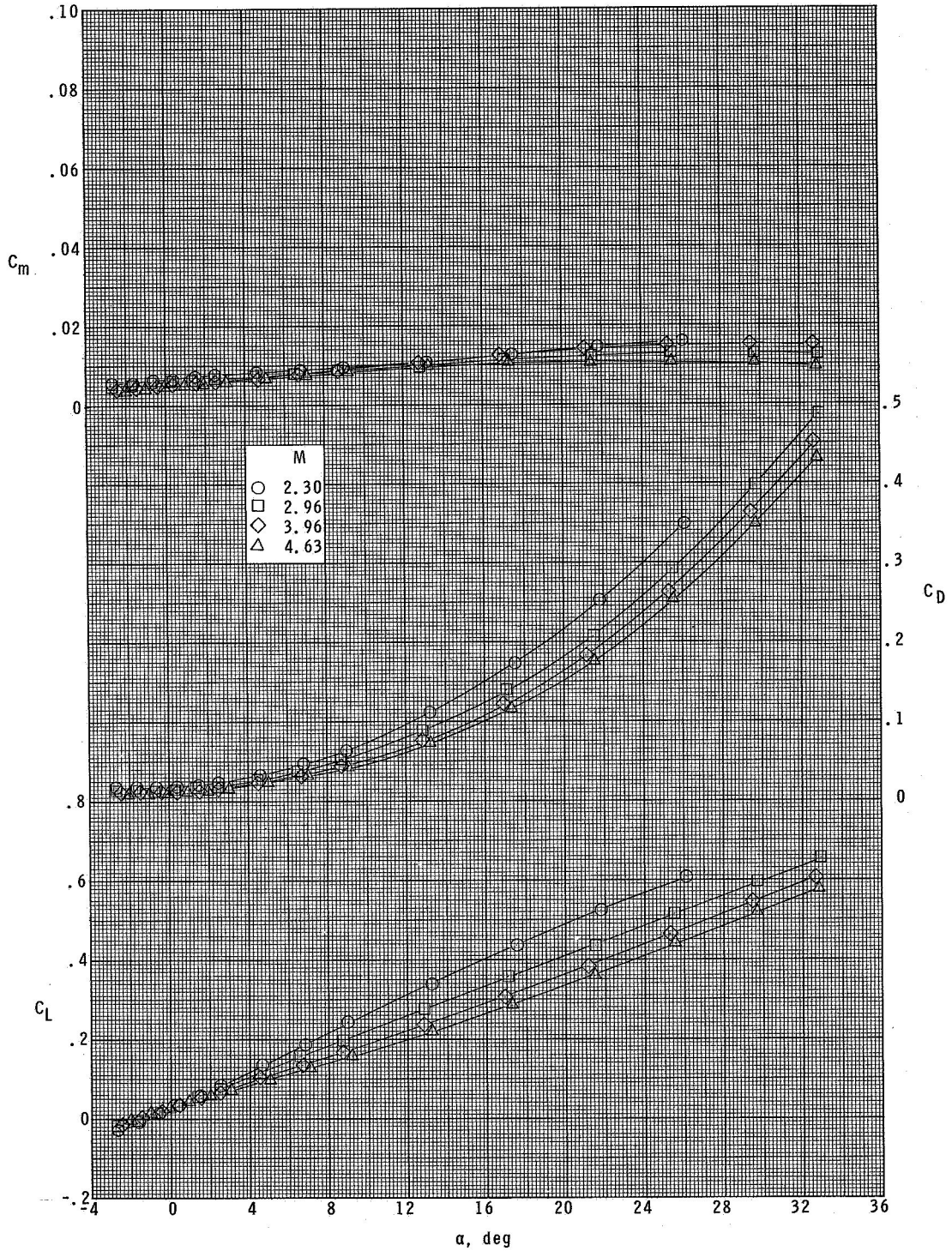

(e) Model 8.

Figure 3.- Concluded.

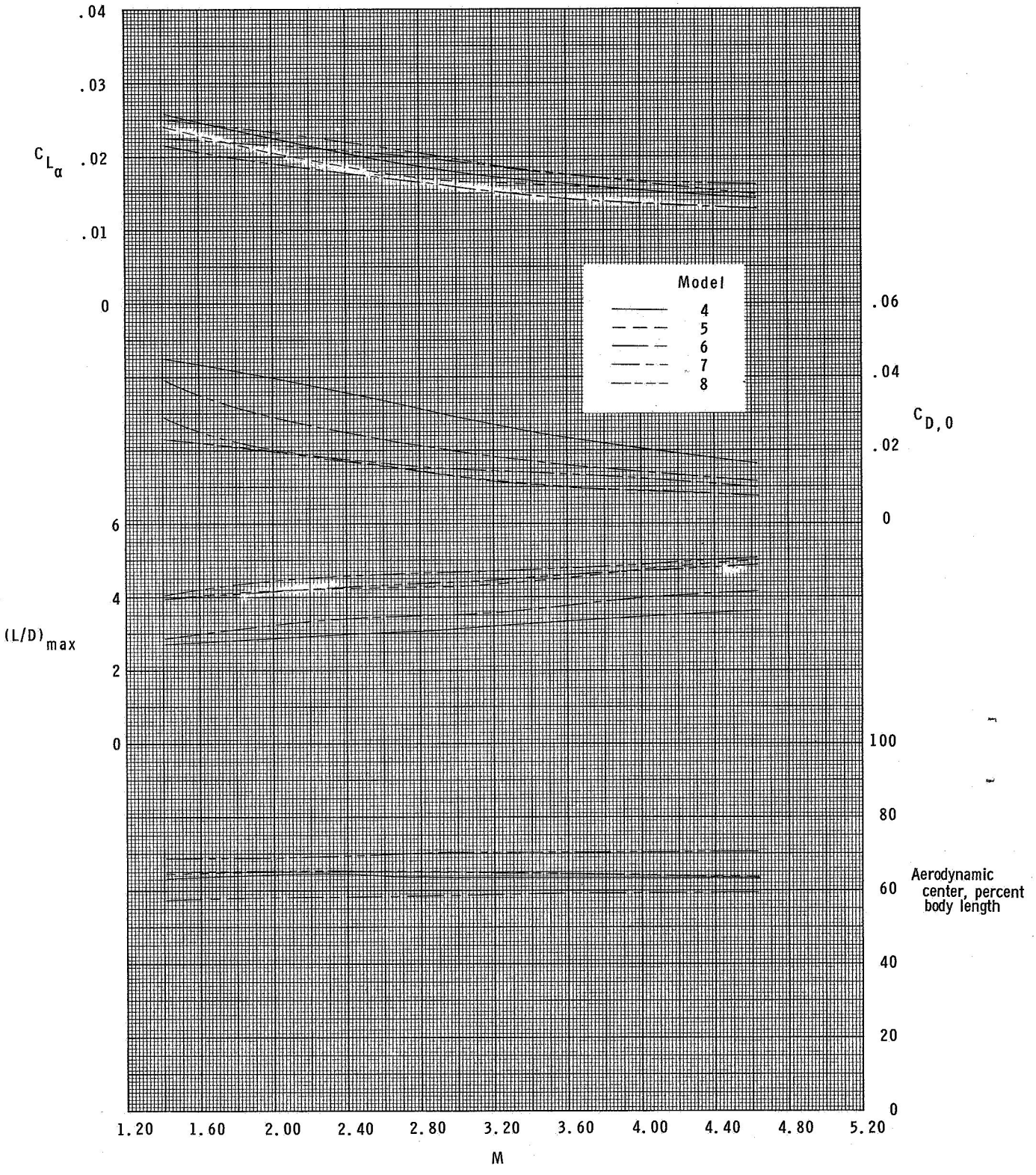

Figure 4.- Summary of longitudinal results. Data for Mach numbers of 1.41 and 2.01 are from reference 1.

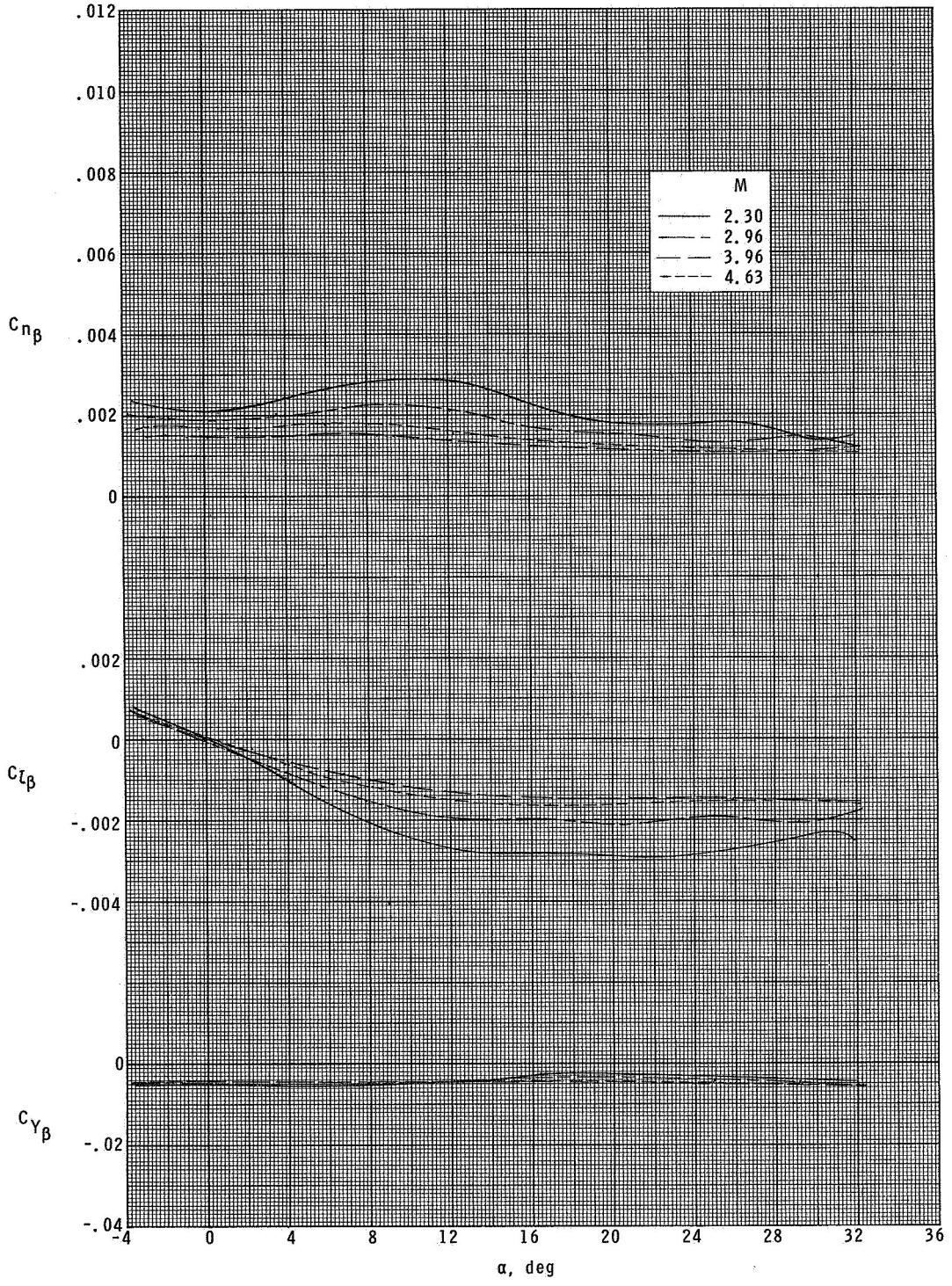

(a) Model 4.

Figure 5.- Variation of lateral parameters with angle of attack.

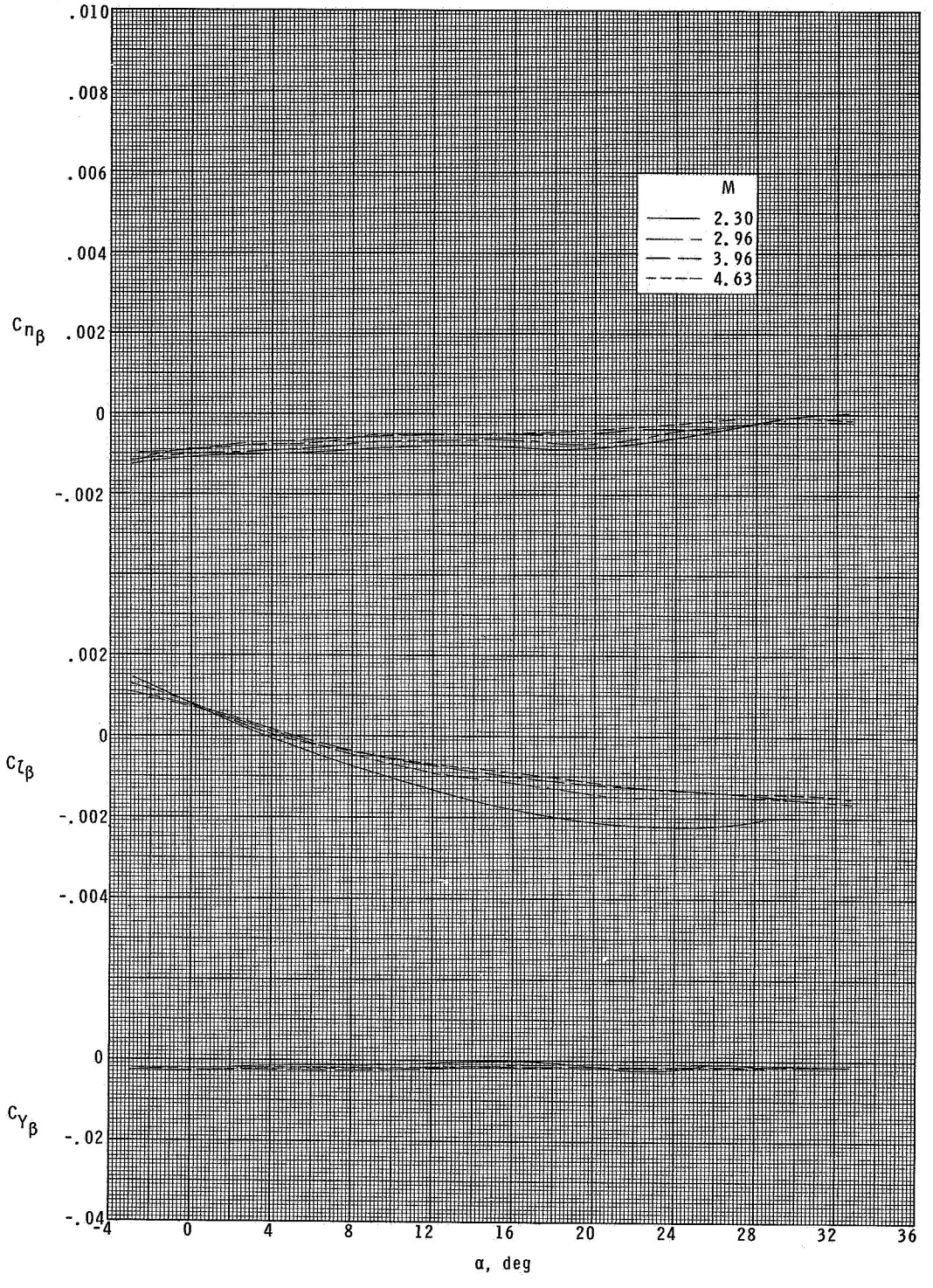

(b) Model 5.

Figure 5.- Continued.

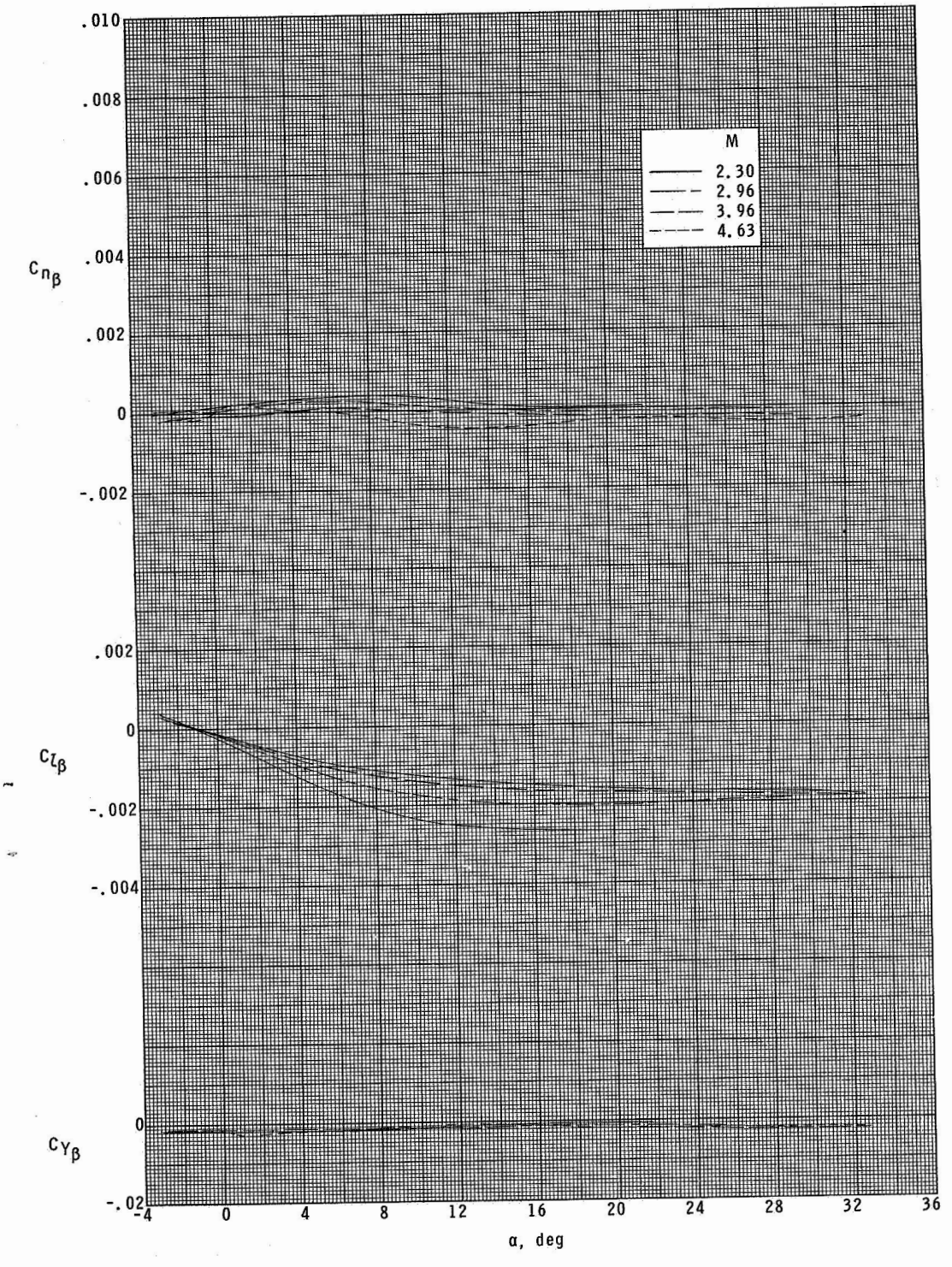

(c) Model 6.

Figure 5.- Continued.

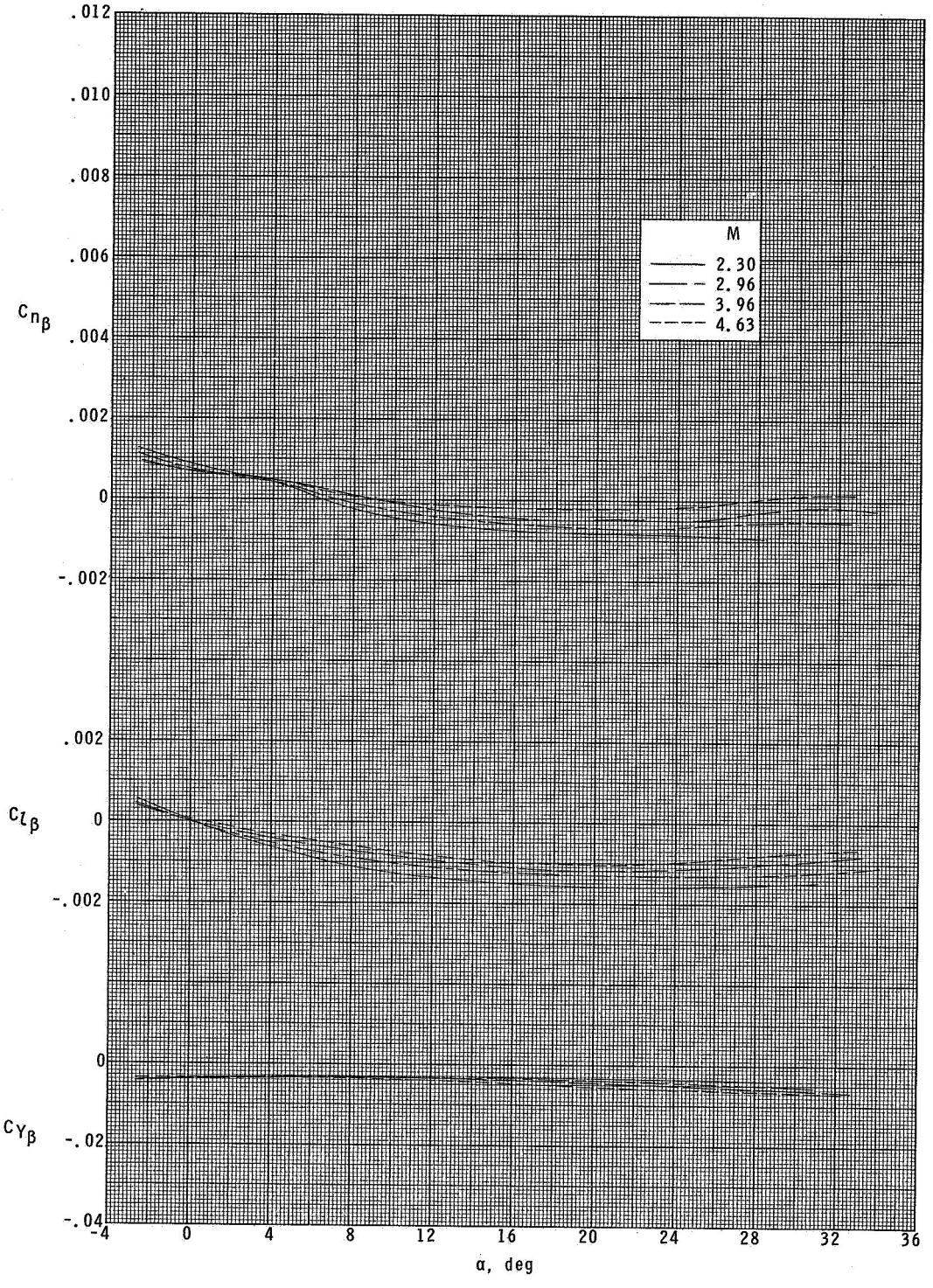

(d) Model 7.

Figure 5.- Continued.

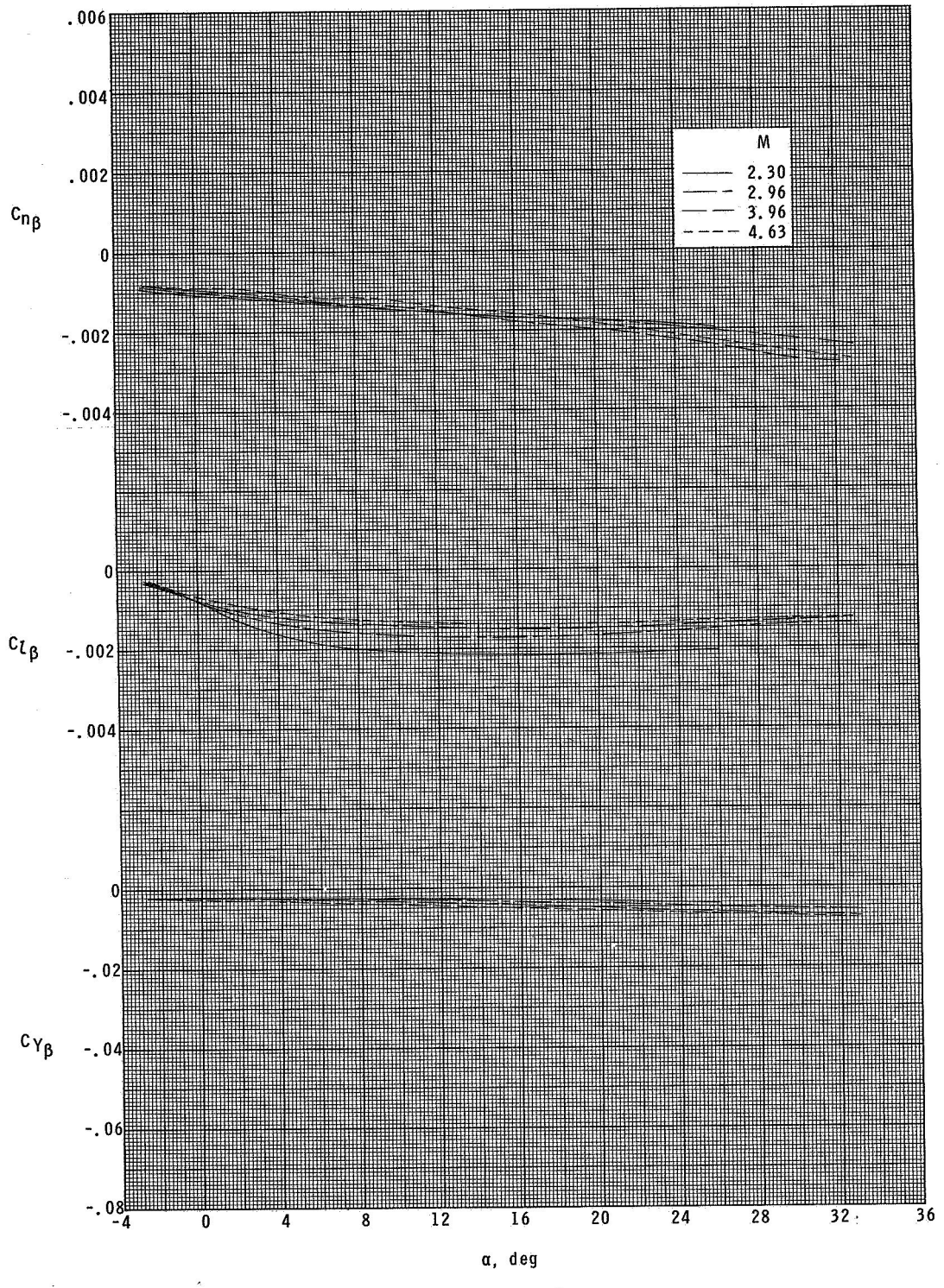

(e) Model 8.

Figure 5.- Concluded.

"The aeronautical and space activities of the United States shall be conducted so as to contribute . . . to the expansion of human knowledge of phenomena in the atmosphere and space. The Administration shall provide for the widest practicable and appropriate dissemination of information concerning its activities and the results thereof."

—NATIONAL AERONAUTICS AND SPACE ACT OF 1958

NASA SCIENTIFIC AND TECHNICAL PUBLICATIONS

TECHNICAL REPORTS: Scientific and technical information considered important, complete, and a lasting contribution to existing knowledge.

TECHNICAL NOTES: Information less broad in scope but nevertheless of importance as a contribution to existing knowledge.

TECHNICAL MEMORANDUMS: Information receiving limited distribution because of preliminary data, security classification, or other reasons.

CONTRACTOR REPORTS: Scientific and technical information generated under a NASA contract or grant and considered an important contribution to existing knowledge.

TECHNICAL TRANSLATIONS: Information published in a foreign language considered to merit NASA distribution in English.

SPECIAL PUBLICATIONS: Information derived from or of value to NASA activities. Publications include conference proceedings, monographs, data compilations, handbooks, sourcebooks, and special bibliographies.

TECHNOLOGY UTILIZATION PUBLICATIONS: Information on technology used by NASA that may be of particular interest in commercial and other non-aerospace applications. Publications include Tech Briefs, Technology Utilization Reports and Notes, and Technology Surveys.

Details on the availability of these publications may be obtained from:

SCIENTIFIC AND TECHNICAL INFORMATION DIVISION
NATIONAL AERONAUTICS AND SPACE ADMINISTRATION
Washington, D.C. 20546